AUG 2 1 2001

0830-L-02 NAS1.29/3-2:01-07

NASA Tech Briefs

National Aeronautics and
Space Administration

Electronic Components and Circuits

Electronic Systems

Physical Sciences

Materials

Computer Programs

Mechanics

Machinery

Fabrication Technology

Mathematics and Information Sciences

Am
2002006930

Life Sciences

C

INTRODUCTION

Tech Briefs are short announcements of innovations originating from research and development activities of the National Aeronautics and Space Administration. They emphasize information considered likely to be transferable across industrial, regional, or disciplinary lines and are issued to encourage commercial application.

Availability of NASA Tech Briefs and TSPs

Requests for individual Tech Briefs or for Technical Support Packages (TSPs) announced herein should be addressed to

National Technology Transfer Center
Telephone No. **(800) 678-6882** or via World Wide Web at **www2.nttc.edu/leads/**

Please reference the control numbers appearing at the end of each Tech Brief. Information on NASA's Commercial Technology Team, its documents, and services is also available at the same facility or on the World Wide Web at **www.nctn.hq.nasa.gov**.

Commercial Technology Offices and Patent Counsels are located at NASA field centers to provide technology-transfer access to industrial users. Inquiries can be made by contacting NASA field centers and program offices listed below.

NASA Field Centers and Program Offices

Ames Research Center
Carolina Blake
(650) 604-1754 or
cblake@mail.arc.nasa.gov

Dryden Flight Research Center
Jenny Baer-Riedhart
(661) 276-3689 or
jenny.baer-riedhart@dfrc.nasa.gov

Goddard Space Flight Center
George Alcorn
(301) 286-5810 or
galcorn@gsfc.nasa.gov

Jet Propulsion Laboratory
Merle McKenzie
(818) 354-2577 or
merle.mckenzie@jpl.nasa.gov

Johnson Space Center
Hank Davis
(281) 483-0474 or
henry.l.davis1@jsc.nasa.gov

John F. Kennedy Space Center
Jim Alberti
(321) 867-6224 or
Jim.Alberti-1@ksc.nasa.gov

Langley Research Center
Sam Morello
(757) 864-6005 or
s.a.morello@larc.nasa.gov

Glenn Research Center
Larry Viterna
(216) 433-3484 or
cto@grc.nasa.gov

George C. Marshall Space Flight Center
Vernotto C. McMillan
(256) 544-2615 or
vernotto.mcmillan@msfc.nasa.gov

John C. Stennis Space Center
Kirk Sharp
(228) 688-1929 or
technology@ssc.nasa.gov

NASA Program Offices
At NASA Headquarters there are seven major program offices that develop and oversee technology projects of potential interest to industry:

Carl Ray
Small Business Innovation Research Program (SBIR) & Small Business Technology Transfer Program (STTR)
(202) 358-4652 or
cray@mail.hq.nasa.gov

Dr. Robert Norwood
Office of Commercial Technology (Code RW)
(202) 358-2320 or
rnorwood@mail.hq.nasa.gov

John Mankins
Office of Space Flight (Code MP)
(202) 358-4659 or
jmankins@mail.hq.nasa.gov

Terry Hertz
Office of Aero-Space Technology (Code RS)
(202) 358-4636 or
thertz@mail.hq.nasa.gov

Glen Mucklow
Office of Space Sciences (Code SM)
(202) 358-2235 or
gmucklow@mail.hq.nasa.gov

Roger Crouch
Office of Microgravity Science Applications (Code U)
(202) 358-0689 or
rcrouch@hq.nasa.gov

Granville Paules
Office of Mission to Planet Earth (Code Y)
(202) 358-0706 or
gpaules@mtpe.hq.nasa.gov

NASA TechBriefs

National Aeronautics and
Space Administration

July 2001
01-07

5 Electronic Components and Circuits

9 Electronic Systems

17 Physical Sciences

23 Computer Programs

27 Mechanics

31 Machinery

35 Mathematics and Information Sciences

41 Life Sciences

This document was prepared under the sponsorship of the National Aeronautics and Space Administration. Neither the United States Government nor any person acting on behalf of the United States Government assumes any liability resulting from the use of the information contained in this document, or warrants that such use will be free from privately owned rights.

4

BLANK PAGE

Electronic Components and Circuits

Hardware, Techniques, and Processes

7 Back-Illuminated CCDs With Integral Ultraviolet-Pass Filters

7 MQW Based Blocked Intersubband Detector for Low-Background Operation

BLANK PAGE

Back-Illuminated CCDs With Integral Ultraviolet-Pass Filters

Filters would be grown directly on silicon device back surface.

NASA's Jet Propulsion Laboratory, Pasadena, California

Efforts are under way to develop back-surface-illuminated, thinned silicon charge-coupled devices (CCDs) with delta doping and integral optical filters to be used as image detectors in the ultraviolet wavelength range. The concept of delta doping of back-surface-illuminated, thinned silicon CCDs as part of an overall design to make CCDs sensitive to ultraviolet light is not new in itself. Delta-doped CCDs were invented at NASA's Jet Propulsion Laboratory in 1992, and it is well established that this process produces ultraviolet-sensitive CCDs with stable and uniform 100-percent internal quantum efficiency. The novelty lies in the proposed fabrication of such CCDs in which both delta doping and optical filter layers would be deposited as integral parts of unitary device structures.

Because silicon CCDs are sensitive to visible light, one of the major challenges in the development of ultraviolet imaging CCDs is to satisfy the need for filters that will reject visible light but pass ultraviolet light. Another major challenge is posed by the fact that the naturally-formed SiO_2 on the air-exposed Si surfaces absorbs light strongly at wavelengths < 140 nm. Hence, it would be desirable to eliminate the SiO_2 layers as well as to deposit visible-light-rejecting filters and antireflection layers on the back surfaces of the CCDs.

The use of integral filters (as distinguished from external filters that are fabricated on separate substrates) would (1) increase the robustness of image detectors by eliminating the external filters, which are delicate; (2) eliminate the need for structural supports for the filters; (3) eliminate the need for the substrates on which external filters are constructed and which introduce optical losses that degrade detector responses at short wavelengths; and (4) reduce the number of optical surfaces, thereby reducing overall optical losses by eliminating the loss (typically at least 2 to 3 percent) associated with each such surface eliminated.

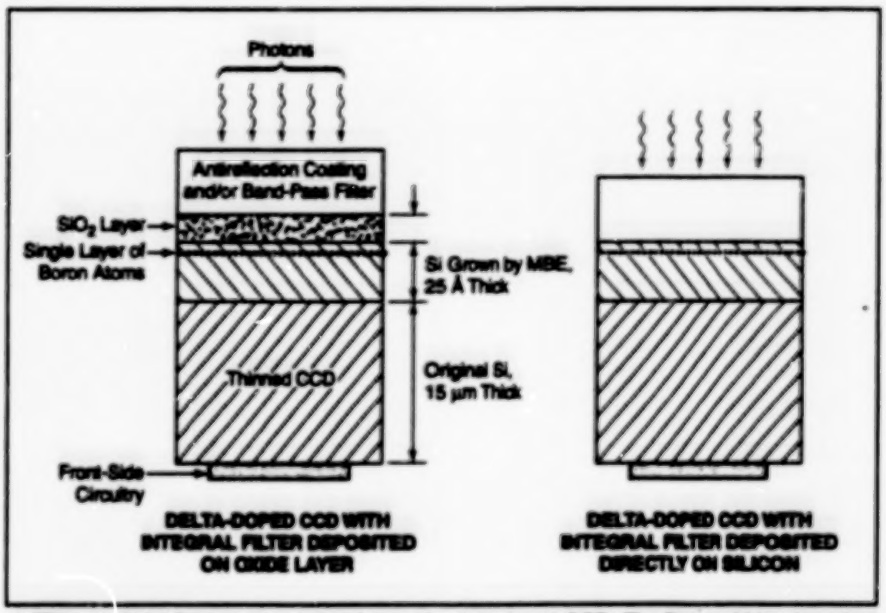
Photons
Antireflection Coating and/or Band-Pass Filter
SiO_2 Layer
Single Layer of Boron Atoms
Si Grown by MBE, 25 Å Thick
Thinned CCD
Original Si, 15 μm Thick
Front-Side Circuitry
DELTA-DOPED CCD WITH INTEGRAL FILTER DEPOSITED ON OXIDE LAYER
DELTA-DOPED CCD WITH INTEGRAL FILTER DEPOSITED DIRECTLY ON SILICON

A Filter would be formed as an integral part of a delta-doped CCD. The filter could be deposited on the back-surface oxide, but it would be preferable to prevent the formation of the oxide and deposit the filter in direct contact with the silicon.

Because the delta-doped layer lies permanently ~5–10 Å beneath the back surface of a CCD, the delta doping process does not pose an impediment to the subsequent deposition of optical filters and antireflection layers. The problem then becomes one of depositing these optical layers directly on the silicon surface, without the formation of an intervening SiO_2 layer. The approach taken in the present development effort is to perform delta doping in one ultrahigh vacuum molecular-beam epitaxy (MBE) chamber and then, without breaking vacuum, transfer the CCD to a connected metal/insulator MBE chamber wherein the filter layers are deposited. By refraining from breaking vacuum until after the deposition of the filter layers, one can prevent the formation of the SiO_2 layer (see figure). At the time of reporting the information for this article, MgF_2 antireflection layers optimized for the wavelength range of 200 to 300 nm had been deposited on delta-doped CCDs and were found to result in modest increase in the quantum efficiency of the CCDs at a wavelength of 180 nm.

This work was done by Shouleh Nikzad, Peter Dessman, Paula Grunthaner, Frank Grunthaner, Michael Hoenk, and R.W. Terhune of Caltech for **NASA's Jet Propulsion Laboratory.** *Further information is contained in a TSP [see page 1].*

In accordance with Public Law 96-517, the contractor has elected to retain title to this invention. Inquiries concerning rights for its commercial use should be addressed to

Technology Reporting Office
JPL
Mail Stop 249-103
4800 Oak Grove Drive
Pasadena, CA 91109
(818) 354-2240

Refer to NPO-21007, volume and number of this NASA Tech Briefs issue, and the page number.

MQW Based Blocked Intersubband Detector for Low-Background Operation

The basic design is modified to suppress space-charge buildup and its deleterious effects.

NASA's Jet Propulsion Laboratory, Pasadena, California

Multiple-quantum-well (MQW) $Al_xGa_{1-x}As$/GaAs infrared photodetectors that are better suited [relative to prior $Al_xGa_{1-x}As$/GaAs quantum-well infrared photodetectors (QWIPs)] for operation under low-background conditions are undergoing development. These devices are expected to function at a temperature of 30 K without nonlinear effects or delayed responses. Even at this low temperature, the readout electronic circuits for imaging arrays of these photodetectors are expected to

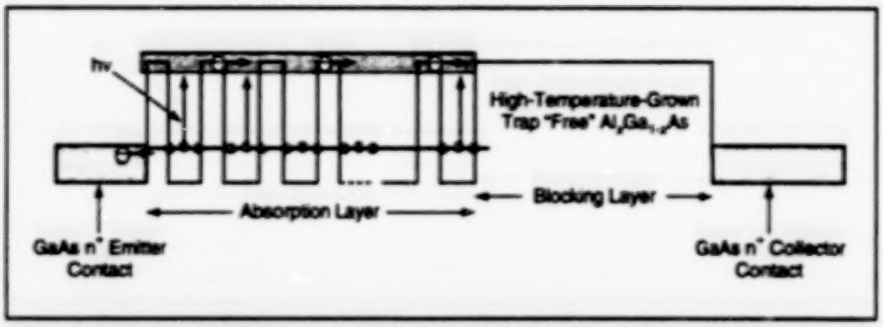

This is an Energy-Level Diagram of an MQW device designed for improved performance under low-background conditions. The device exploits tunneling between the negative n⁺ GaAs contact layer and the wells in the MQW emitter section for ultra fast replenishment of depleted wells, while the thick undoped $Al_xGa_{1-x}As$ barrier layer suppresses undesired tunneling between the MQW emitter section and the positive n⁺ GaAs contact layer. (Note: h=Planck constant; ν = frequency of radiation.)

work smoothly — that is, with no freezeout of charge carriers. Large focal-plane arrays of these detectors should be relatively inexpensive because they could be fabricated by use of mature techniques for the growth and processing of $Al_xGa_{1-x}As/GaAs$.

Some background information is prerequisite to a meaningful description of the present MQW photodetectors: The operation of QWIPs is based on photoexcitation of electrons between ground and first-excited-state subbands of quantum wells, which are formed by stacking alternate layers of two different, high-bandgap semiconductor materials (e.g., $Al_xGa_{1-x}As$ and GaAs). The discontinuity in bandgaps between the two materials gives rise to quantized subbands in the potential wells associated with conduction bands. The parameters of the layers are chosen so that photoexcited charge carriers can escape from the potential wells and be collected as photocurrent. Thus, in principle, a QWIP operates similarly to an extrinsic bulk photoconductor.

Electrons in the subbands of the isolated quantum wells in a typical prior QWIP can be visualized as electrons attached to impurity states in bulk photoconductors. As a photogenerated electron leaves the active doped quantum-well region, it leaves behind a hole that constitutes an increment of space charge. For operation under low-background conditions, QWIPs are designed to have extremely low tunneling currents and extremely low thermionically emitted dark currents at low temperature (30 K). Hence, in the event of low background irradiance, the high resistivity of the active region (a consequence of the large thickness of the barriers between wells) can lead to a delay in refilling the wells. This delay, in turn, results in a decrease in responsivity with an increase in the frequency of intensity modulation of the infrared radiation that one seeks to detect. This frequency response is similar to that associated with dielectric relaxation in bulk photoconductors. This completes the background information.

The developmental MQW based Block Intersubband Detectors (BID) are designed to suppress the deleterious effects described above. A device of this type (see figure) includes a heavily doped MQW emitter section with barriers that are thinner than in prior QWIP devices. The thinning of the barriers results in a large overlap of sublevel wave functions, thereby creating a miniband. Because of sequential resonant quantum-mechanical tunneling of electrons from the negative ohmic contact to and between wells, any space charge is quickly neutralized. At the same time, large tunneling current through the whole device is suppressed by a relatively thick, undoped $Al_xGa_{1-x}As$ layer between the MQW emitter section and the positive ohmic contact. [This layer is similar to the thick, undoped silicon layers used in the block impurity band (BIB) type.]

This work was done by Sarath Gunapala, Sumith Bandara, John K. Liu, Sir B. Rafol, David Ting, and Jason Mumolo of Caltech for **NASA's Jet Propulsion Laboratory**. *Further information is contained in a TSP (see page 1).*

In accordance with Public Law 96-517, the contractor has elected to retain title to this invention. Inquiries concerning rights for its commercial use should be addressed to

Technology Reporting Office
JPL
Mail Stop 249-103
4800 Oak Grove Drive
Pasadena, CA 91109
(818) 354-2240

Refer to NPO-21073, volume and number of this NASA Tech Briefs *issue, and the page number.*

Electronic Systems

Hardware, Techniques, and Processes

11 The Wireless Augmented Reality Prototype Concept

12 Common-Path Heterodyne Interferometers

13 System Processes Data From Wind-Tunnel Acoustic Measurements

14 Airfield Wind Advisory Systems for General Aviation

BLANK PAGE

The Wireless Augmented Reality Prototype Concept

Head- and belt-mounted units would enable wearers to communicate data.

NASA's Jet Propulsion Laboratory, Pasadena, California

The Wireless Augmented Reality Prototype (WARP) is a system for personal access to a local area network with video, audio, and sensor data services. The center of the WARP system is a lightweight, unobtrusive heads-up display with a wireless wearable control unit, called the Remote Access Unit (RAU). Data services to the RAU are provided through a high-rate radio link from the WARP RAU to a stationary base-station interface unit which sits on an ordinary local area network. The RAU-to-interface unit radio link has been engineered to operate within the high-interference, high-multipath environment of a space shuttle or space station module.

The key to WARP is the streamlining and miniaturization of the wearable RAU, allowing long-term use without battery replacement or continuous re-loading of new data. This has been accomplished by paring the RAU electronics down to include only highly integrated video and audio compression/decompression and data multiplexing circuits along with a high-rate two-way radio link. This approach not only allows real-time video and audio conferencing through WARP, but also removes the requirement for information to be stored in the wearable unit. Instead, the most up-to-date and directly relevant data may be retrieved on demand, as real-time situations dictate.

One of the major technology challenges with this concept has been to provide wireless high-rate information in the environment of a space module. Tight confines, metal walls, and lack of radio absorbers create an enormous potential for destructive self-interference. The development of this radio technology is synergistic with the development of technology for efficient and high-quality video data compression; the WARP communications channel contains video, audio, and sensor data simultaneously.

In the space station applications, a virtual terminal is provided by a RAU and headset pair. The user will be able to view and manipulate imagery, text or video, using voice commands to control the terminal operations. WARP hands-free access to computer-based instruction texts, diagrams, and checklists replaces juggling manuals and clipboards and tetherless computer system access allows free motion throughout a cabin while monitoring and operating equipment.

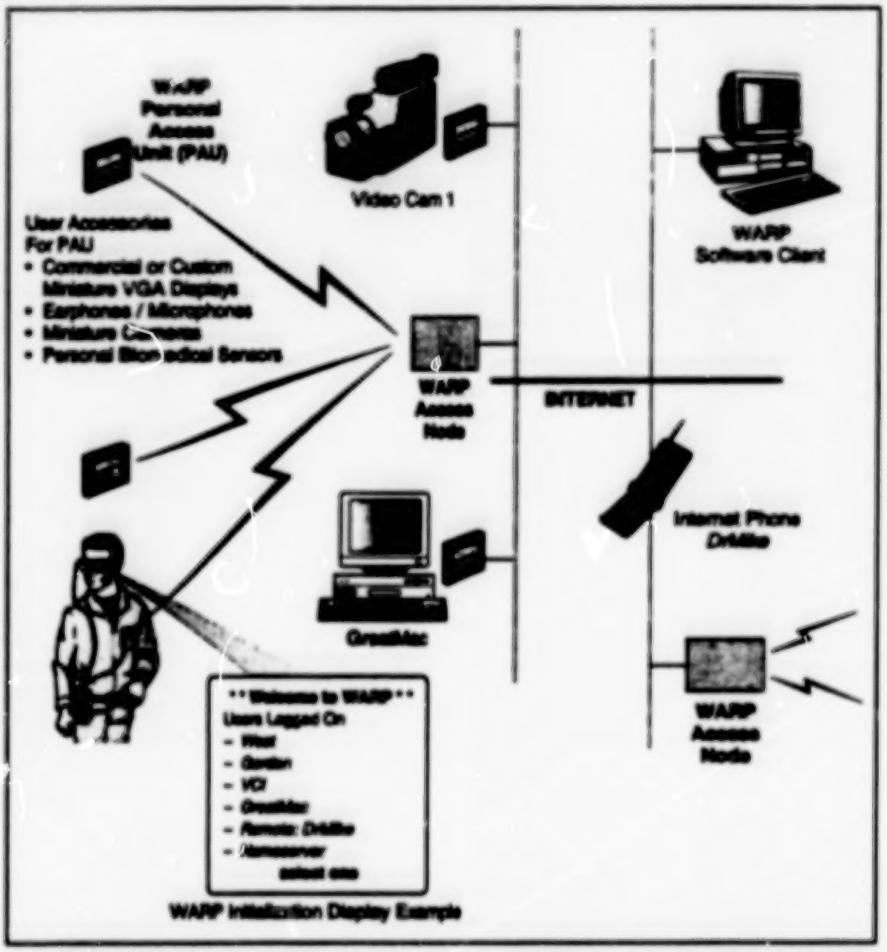

The Wearer Would Interact With a Computer in a base station. Through voice commands, the wearer would control some functions of the computer. The head-mounted display terminal would serve as a remote display device of the computer.

Along with information provided to the astronaut, WARP also allows external observation of the astronaut's situation; personal biosensors connected to the RAU can send back continuous telemetry and a miniature camera integrated into the headset provides real-time video of the wearer's field of view. In this way, for example, a principal investigator located on Earth may consult with a payload specialist on the operation or troubleshooting of the equipment. Using this same mechanism, WARP RAUs may also be used with stand-alone wireless sensor packages that send data, from low-rate environmental sensors or high-rate cameras, back through the existing WARP wireless network to the base station. Packetized data may be sent to various monitor computers for logging or alarm.

Future applications of WARP are in any environment where heads-up, hands-free information retrieval — and remote situational awareness — improves efficiency, including field operations, tetherless operations/monitor consoles, remote consultations in medical or maintenance procedures, and hazardous or confined-space activities. The extension of WARP system and RAUs into a wireless SensorNet is a novel approach to space or air vehicle infrastructures, saving mass and providing flexibility over hard-wired sensor or camera installations.

The WARP program has built and integrated several Phase II WARP systems. The Phase II system supports single, inde-

pendent RAU-to-base station connections to a single PC. Phase II WARP is under evaluation at Johnson Space Center. Development is now underway on Phase III WARP, which will allow each interface unit to network multiple RAUs, and will allow individual RAUs to be supported dynamically by multiple interface units which are installed in a cellular network type model throughout an extended area.

This work was done by Martin Agan, Ann S. Devereaux, and Thomas Jedrey of Caltech for **NASA's Jet Propulsion Laboratory**. *Further information is contained in a TSP [see page 1].*

In accordance with Public Law 96-517, the contractor has elected to retain title to this invention. Inquiries concerning rights for its commercial use should be addressed to

Technology Reporting Office
JPL
Mail Stop 249-103
4800 Oak Grove Drive
Pasadena, CA 91109
(818) 354-2240

Refer to NPO-20621, volume and number of this NASA Tech Briefs issue, and the page number.

Common-Path Heterodyne Interferometers

These are expected to perform better than do phase-shifting interferometers.

NASA's Jet Propulsion Laboratory, Pasadena, California

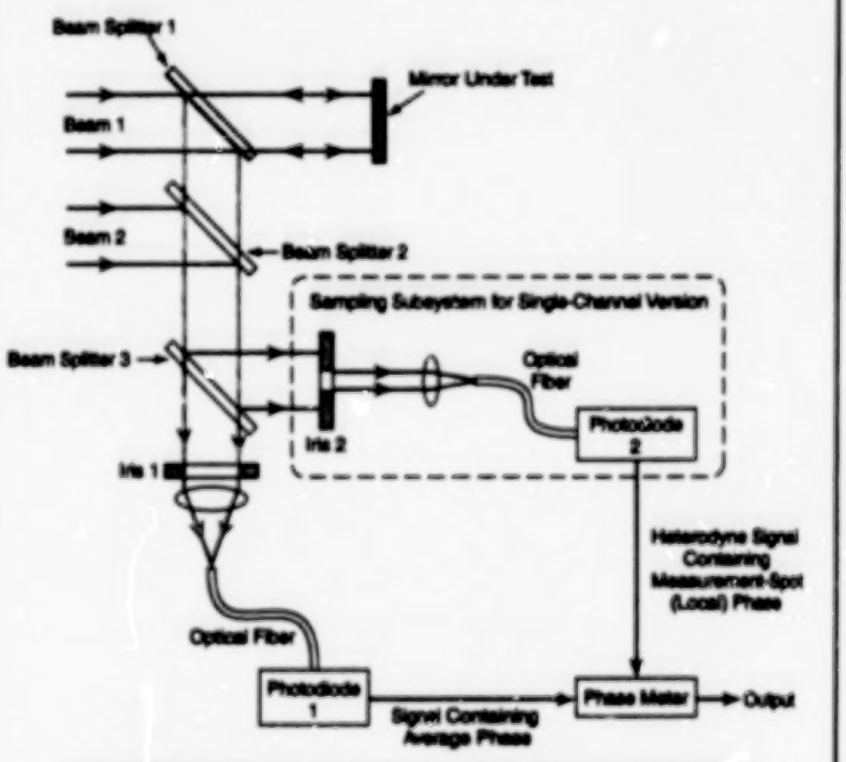

SIMPLIFIED DIAGRAM OF A COMMON-PATH HETERODYNE INTERFEROMETER

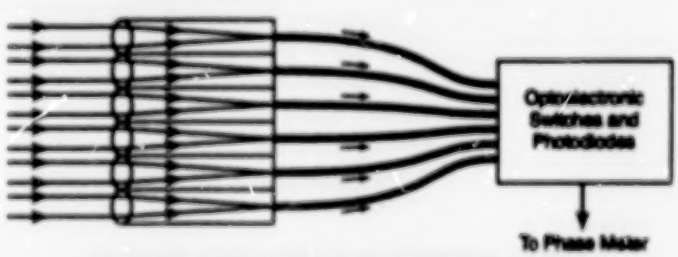

SAMPLING SUBSYSTEM FOR MULTICHANNEL VERSION

A Common-Path Heterodyne Interferometer could generate a high-resolution surface-height map of a mirror surface under test. A multichannel version would be capable of sampling the surface under test in a relatively short time.

Common-path heterodyne interferometers (COPHIs) have been proposed for measuring small variations in the heights of surfaces. A COPHI could be used, for example, to measure the deviation of the surface of a mirror or other optical component from nominal flatness or nominal sphericity. Like phase-shifting interferometers that have been used previously for the same purpose, a COPHI would generate an optical-phase map equivalent to a topographical map of the surface under test. The advantages of the COPHI over a phase-shifting interferometer would be (1) greater resolution in phase and thus in surface height and (2) shorter measurement time.

The figure depicts a COPHI for measuring the deviation of a mirror from flatness. The light from a laser would be split into two coherent beams, denoted 1 and 2. By use of an acousto-optical modulator, beam 1 would be modulated at a radio frequency f_1. In the same manner, beam 2 would be modulated at frequency f_2, which would differ from f_1 by a convenient amount, e.g., 10 kHz. Half of beam 1 would pass through beam splitter 1. The mirror under test would be positioned to retro-reflect beam 1. After reflecting off beam splitter 1, beam 1 would combine with beam 2 at beam splitter 2 to form interference fringes.

The interference fringe would then be split into two identical sets with beam splitter 3. One set of fringe would pass through a large iris 1, which would sample the entire portion of the mirror surface. The light would be coupled into and through an optical fiber to photodiode 1; consequently, the phase of the $|f_1 - f_2|$ frequency heterodyne output of photodiode 1 would amount to an average over the entire mirror surface. This heterodyne output would be used as a reference signal (REF). The other set of fringe would then pass through a much smaller iris 2, which would select a small spot on the mirror for measurement. After passing through iris 2, the light would be coupled into and through a second fiber to photodiode 2. This heterodyne output would be used as measurement signal (UNK). The phase of the $|f_1 - f_2|$ frequency heterodyne output of photo-

diode 2 would thus correspond to the surface height at the measurement spot.

A high-resolution phase meter would measure the phase difference between UNK and REF, thus providing a measurement of the deviation of the measurement-spot surface height from the average surface height of the mirror. Because of the common path nature of REF and UNK signals, many error sources such as vibration would become common-mode error in the measurement. This interferometer configuration would allow much higher resolution than phase-shifting interferometers.

A surface-height map of the test surface could be generated from phase readings acquired in a mechanical scan of iris 2. Of course, such a scan would take some time. To eliminate the need for mechanical scanning, one could construct a multichannel version of the COPHI. Iris 2 would be replaced by a 2-D array of pinlets registered with input ends of many optical fibers. Each optical fiber would define a pixel in the interference image of the test surface. The output ends of the optical fibers would be connected via an optoelectronic switch to a smaller number of photodiodes. By a combination of electronic and optoelectronic switching, the outputs of the photodiodes would be fed sequentially to the phase meter to generate a sequence of phase readings, each corresponding to one pixel.

This work was done by Feng Zhao of Caltech for **NASA's Jet Propulsion Laboratory.** *Further information is contained in a TSP [see page 1].*

NPO-20786

System Processes Data From Wind-Tunnel Acoustic Measurements

This system is a powerful aid for aircraft-noise-reduction research.

Ames Research Center, Moffett Field, California

A processing system has been developed to meet increasing demands for detailed noise measurement of aircraft in wind tunnels. Phased arrays enable spatial and amplitude measurements of acoustic sources, including low signal-to-noise sources not measurable by conventional techniques. The Microphone Array Phased Processing System (MAPPS) provides processing and visualization of acoustic array measurements made in wind tunnels. The system uses networked parallel computers to provide noise maps at selected frequencies in a near real-time testing environment. The system has been successfully used in two subsonic, hard-walled wind tunnels, the NASA Ames 7- by 10-Foot Wind Tunnel and the NASA Ames 12-Foot Wind Tunnel. Low-level airframe noise that cannot be measured with traditional techniques was measured in both tests.

The MAPPS system is an end-to-end system designed to be used by researchers. MAPPS begins at the end of the data acquisition and storage and ends with the processed data visualization. This system is designed to be versatile and robust in its treatment of variable numbers of microphones, number and locations of processors, versatile calibrations, and visualization requirements. This versatility is designed into the system to provide for alternatives if components fail. These component failures will result in degraded results, but the results will still provide the researcher with information to meet their needs. MAPPS provides ease of use for processing and visualization with its system approach and graphical user interface (GUI). The system is designed so that the user may concentrate on research, testing, and data interpretation, instead of data and file manipulation.

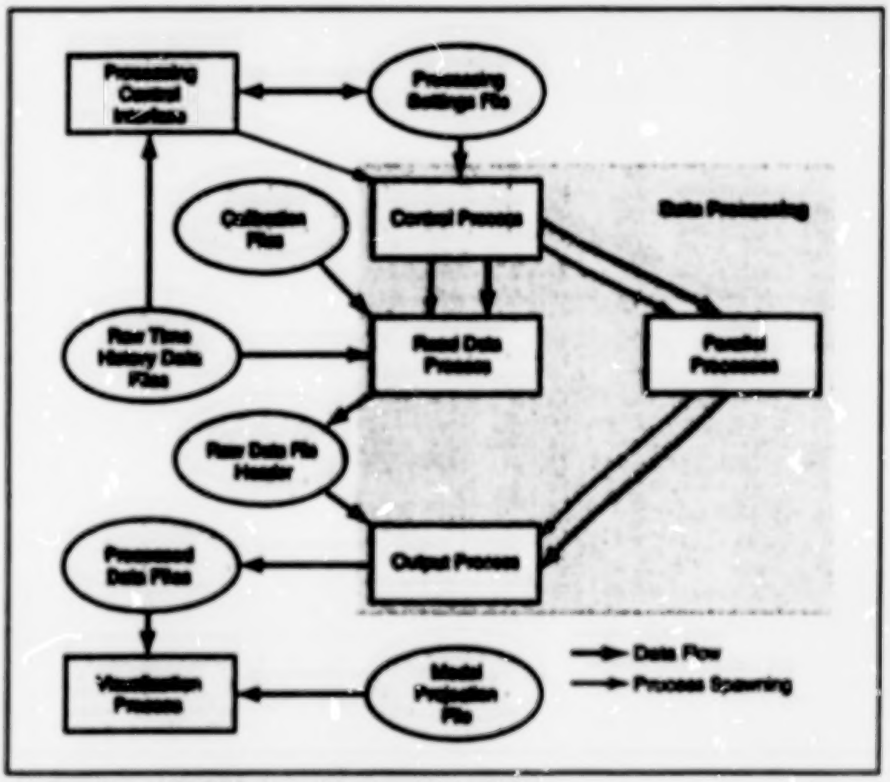

An Overview of MAPPS shows key processing activities.

An operational design goal for MAPPS was to provide sufficient results in near-real-time to allow the test director and researcher to make future run content decisions. The first operational test of MAPPS was in a recent Flap Edge test using a 100-element microphone array in the NASA Ames 7- by 10-Foot Wind Tunnel. The system met a 9-minute cycle from end of data acquisition to showing results on screen for 166 frequencies with 400 averages and a frequency resolution of 150 Hz. This cycle time was sufficient to obtain results from a small number of points for each run condition and to allow the test director to make model change and run condition decisions for the next run. Another operational design consideration was to have all the data processed and ready for examination by the next day. The ability to batch process multiple data points was also demonstrated at this test.

The MAPPS system (see figure) starts with a raw time history and produces a processed data file and computer visualization of the results. The input raw data file and the output processed data file are both stored in a widely-used self-describing, machine-independent binary file format called Network Common Data Format. Besides the basic data, these data files contain all the information related to the instrumentation, test setup, and

test conditions. MAPPS includes many files and computer programs. The user sets all the processing parameters and initiates interactive processing through the Processing Control interface. The Processing Control interface reads the header information in the Raw Time History Data File. Processing parameters may be used from a file or set interactively based upon information derived from the header and displayed in the interface. All the processing parameters are saved in the Process Settings File. The data processing occurs in four processes that run without user interaction once the Processing Control Interface or a UNIX script for batch processing starts the Control Process. The computer running the Control Process must have access to the Processing Settings File that was written by the Processing Control Interface. The Read Data Process must have access to the Calibration File(s) and the Raw Time History Data File. When processing is complete, the Output Process writes the results and header to the Processed Data File. The header of the Processed Data File contains all the information from the header of the Raw Time History Data File plus all of the parameters used to process the data. Data visualizing is done in a separate process. Visualization requires access to the Processed Data File and Model Projection File.

Efficient and versatile visualization of array results is an essential part of MAPPS. MVIEW is a data visualization program written at Ames Research Center to view data processed with MAPPS. Scan results can also be loaded into the DARWIN system. This system allows searching of the database for desired test conditions and performing preliminary looks at the array results. Researchers can then use MVIEW to investigate the desired test conditions in more detail.

Several types of data can be viewed in MVIEW. An overview plot contains three curves displaying the average level of all the good microphones, the maximum level found in the scan and the average level found in the scan as functions of frequency. This plot of curves assists the user in determining which frequency data to view in detail. Other plot windows display the scan maps of noise sources and model in two- and three-dimensional views. The scanned sources are displayed as colored maps and/or contours. The user can control the scale on the map. The scan maps can also be animated to display results for successive frequencies to run like a movie by clicking on the start animation button in the overview plot window.

This work was done by Michael E. Watts and Marianne Mosher of **Ames Research Center** *and Jorge Barulina and Michael Barnes of Caelum Research Corp. Further information is contained in a TSP [see page 1].*

Inquiries concerning rights for the commercial use of this invention should be addressed to the Patent Counsel, Ames Research Center, (650) 604-5104. Refer to ARC-14258.

Airfield Wind Advisory Systems for General Aviation

These systems reduce risks associated with unknown winds during takeoffs and landings.

Dryden Flight Research Center, Edwards, California

An Airfield Wind Advisory System (AWAS) includes a self-contained weather station, located at an airfield, that measures speed and direction of the wind, the temperature, the barometric pressure, and the humidity. This ground station digitizes these measurements and transmits the measurement data in real time, via radio, to portable units in aircraft cockpits. The portable units automatically detect the data and display the information to pilots. In 1999, a prototype of the AWAS system was demonstrated to function successfully in tests at Kennedy Space Center's Space Shuttle Landing Facility in 1999.

An AWAS ground station is designed for automatic operation with minimal maintenance, using either alternating current from a power line or power from a solar photovoltaic array with battery backup. AWAS ground stations can include solid-state transducers with no sliding parts (e.g., sonic anemometers and/or strain-gauge wind sensors) for high reliability but could also be designed to take advantage of previously installed anemometers, weather vanes, and other weather-measurement devices. AWAS ground stations can also contain Web server computers, which transmit the information to wide-area networks over intranet or Internet links upon demand. The transmitted information can include not only the data from the AWAS weather measurements but also Global Positioning System (GPS) data and/or other geophysical data from measurement devices to support scientific observations.

An AWAS airborne unit includes an antenna, receiver, microprocessor, data-storage elements, a power supply, and a back-lit liquid-crystal display device. The simplest version provides a no-clutter display that can be read by the pilot in a one-second glance, showing the following data:

- The identity of the airfield [represented by a three- or four-character label assigned by the Federal Aviation Administration (FAA) to every airfield or helipad],
- The direction of the wind in degrees measured from magnetic north,
- The steady-state and peak gust wind speeds in knots, and
- The most favorable runway for takeoff and landing.

In order to select the most favorable runway, the microprocessor in the airborne unit compares the wind vector with the runway heading (runway headings are stored in an internal database) and calculates the headwind and crosswind values. The runway indicated on the display device is the one with the highest headwind and lowest crosswind components. A switch enables the pilot to command the display of the headwind and crosswind data for the selected runway.

A standby switch shuts off the display device, but allows the remainder of the airborne unit to operate in a listening mode to conserve energy when not in range of an airfield. Advanced versions may include keypads to enable pilots to select specific airfields or runways or to enter special data or queries.

Specialized AWAS software, which may also be incorporated into wireless personal data assistants (PDAs) and hand-held GPS devices, could provide graphical depictions of airfield diagrams and winds. The Internet version of the AWAS is intended for use with wireless PDAs and cellular telephones that provide access to the Internet.

The AWAS can also be used to disseminate weather information in real time in applications other than aviation. Examples of potential users include the National Weather Service, the military, commercial weather services, marine and agricultural concerns, the Federal Emergency Management Agency, and emergency services (e.g., firefighters during forest fires).

The receiver in an AWAS airborne unit automatically detects the signal from an

AWAS ground unit at an airfield and activates the display device when in range of the airfield. The display helps the pilot to select the optimum approach to the airfield while 8 to 10 miles (about 13 to 16 km) out, thus saving three to five minutes per landing. Under visual flight rules (VFR), approaching an uncontrolled field, the pilot is required to make contact with the UNICOM of the airfield to request wind and runway information (UNICOMs are nongovernment communication facilities that provide airport information at some airports). If there is no answer, as is often the case, the pilot must fly over the airfield to view the windsock while visually avoiding other traffic, estimating the wind speed, and entering the traffic pattern to land, trusting that other pilots are also making the same assumptions about the winds and the landing runway. This procedure typically involves extra maneuvering and backtracking. With the AWAS, the pilot knows the wind at the airfield and knows which runway is most favorable, and is therefore able to fly a more direct approach to the landing pattern, without guesswork or extra maneuvering. More importantly, the pilot knows the headwind and crosswind for each runway without question, and will therefore be able to plan ahead for the appropriate aircraft alignment and control inputs.

According to the Aircraft Owner's and Pilots Association annual aviation safety report for the U.S. (the Nall Report), takeoff and landing accidents are "seldom fatal", but the numbers of such accidents are still considerable. During the year of the 1998 report, there were 743 takeoff and landing accidents, which resulted in 46 fatalities. One can infer that the number worldwide is at least 100 per year. The AWAS can contribute significantly to a reduction in the numbers of such mishaps and fatalities. As shown in the Nall Report for general aviation, the greatest number of accidents by far occurs during the takeoff and landing phases of flight. These two phases require the greatest skill and most intense concentration from the pilot, and occur when the aircraft is closest to the ground, at its most vulnerable maneuvering speed, and with the least amount of maneuvering airspace. Wind conditions are extremely critical during these phases of flight. By having the current wind and gust conditions immediately available, the pilot can mentally prepare the approach or takeoff in advance, and reduce the need for surprise reactions. The AWAS can also reduce the risks associated with practicing crosswind landings by making the wind information always readily available to the student pilot and instructor.

This work was done by Gerald E. Brown and Paul A. Curto of NASA Headquarters and Jan A. Zysko of Kennedy Space Center for **Dryden Flight Research Center**. *Further information is contained in a TSP [see page 1].*

This invention is owned by NASA, and a patent application has been filed. Inquiries concerning nonexclusive or exclusive license for its commercial development should be addressed to the Patent Counsel, Dryden Flight Research Center [see page 1]. Refer to DRC-99-16.

BLANK PAGE

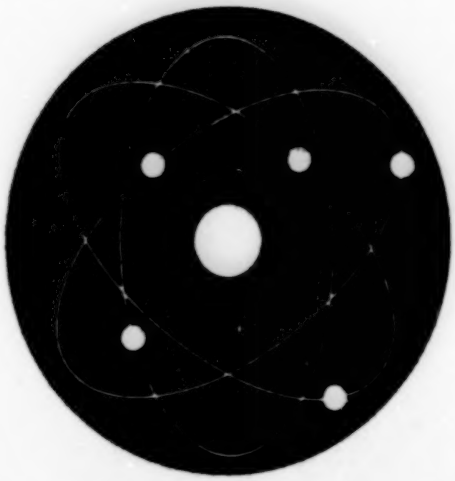

Physical Sciences

Hardware, Techniques, and Processes

19 Infrared Sensors for Detecting Icing on Helicopter Blades
20 Apparatus for Time- and Wavelength-Resolved Spectroscopy
20 Shared-Aperture Multiplexed Holographic Scanning Telescopes

Books and Reports

21 Capture and Escape of Charge Carriers in Quantum Dots
22 Rayleigh-Scattering Measurements in Underexpanded Jets

BLANK PAGE

Infrared Sensors for Detecting Icing on Helicopter Blades

It may be possible to detect icing in a single blade pass.

John H. Glenn Research Center, Cleveland, Ohio

Infrared-sensor systems for real-time detection of accretion of ice on helicopter rotor blades are undergoing development. By providing early warnings of icing conditions, these systems would enable pilots to activate deicing equipment or take other corrective action to avoid the severe hazards posed by icing.

The accretion of ice on a helicopter rotor blade begins and is concentrated at the leading edge. Because the freezing process releases latent heat of fusion, the leading edge becomes warmer than the remainder of the blade surface. The present icing-detection technique is based primarily on infrared measurement of the icing-induced variation of temperature between the leading and trailing edges. Secondarily, the technique also involves the use of infrared signatures to determine whether a blade is dry or whether ice has already accumulated.

A system of the type under development includes an upward-staring infrared sensor mounted on top of a helicopter fuselage (see Figure 1). The sensor measures infrared radiation indicative of the temperature profile across the blade as the blade passes by overhead. Experiments have shown that the optimal sensor for this application is a thermoelectrically cooled PbSe photodetector, which is sensitive to radiation in the wavelength range of 3 to 5 μm. A prototype system that has shown promise in experiments includes such a sensor equipped with a germanium lens to focus on a small spot in the rotor-blade plane, plus electronic circuits for digitizing the sensor readings and processing the digitized readings.

Figure 2 shows infrared-sensor readings taken from three representative helicopter-blade passes during a field test. The curve labeled "Dry" indicates a fairly uniform blade temperature under non-icing conditions. The curve labeled "Icing" was obtained at the commencement of icing caused by the impingement of supercooled water droplets; this curve clearly shows the expected temperature rise at the leading edge. The curve labeled "Static Ice" manifests an apparent cooling of the leading edge after ice had accumulated on the blade but icing conditions were no longer present; this leading-edge-cooling effect is observed consistently under such circumstances and could thus be a basis for detecting ice already present after icing conditions have passed.

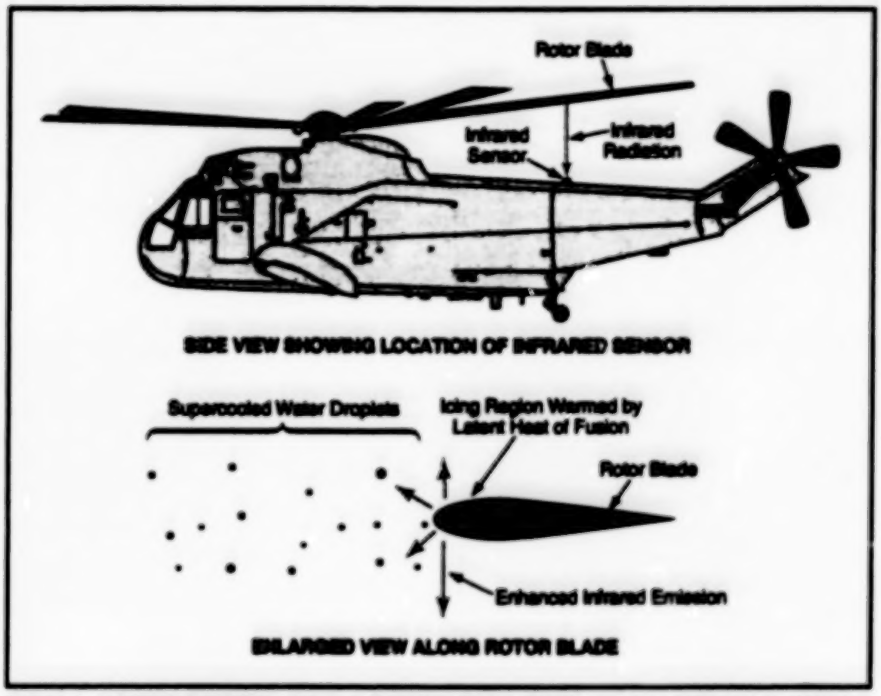

Figure 1. Infrared Radiation From a Passing Rotor Blade can be measured to detect a leading-edge temperature rise indicative of icing.

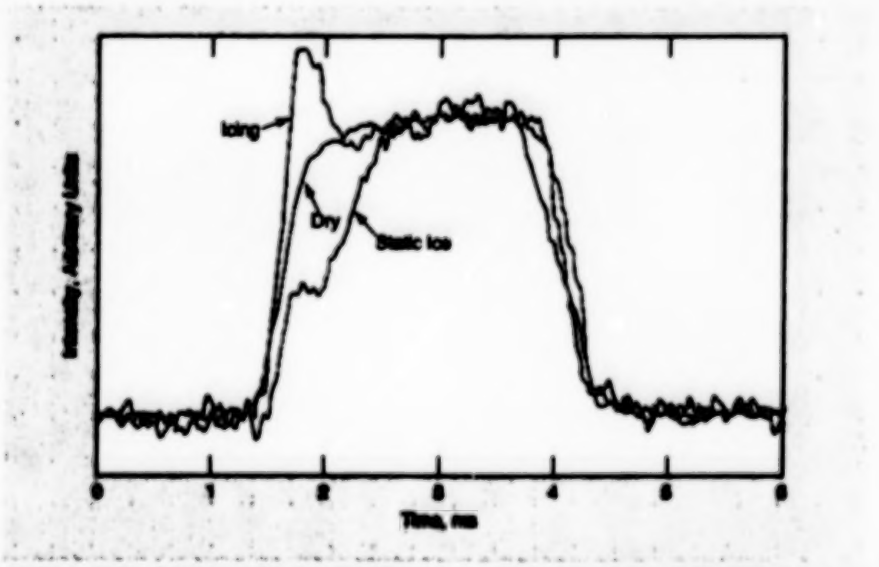

Figure 2. Plots of Infrared-Sensor Readings of a passing rotor blade exhibit distinct shapes indicative of the icing and non-icing conditions under which the readings were taken.

The most noteworthy feature of the infrared blade signatures of Figure 2 is that it is apparently possible to distinguish among the three indicated conditions from a single blade pass — an observation time of the order of 2 ms. Even if an ice-detection system employs an algorithm that processes digitized sensor readings from multiple passes to increase the robustness of the decision as to which of the three conditions has been detected, it should be possible to achieve a response time of the order of 1 s.

This work was done by R. J. Hansman of Massachusetts Institute of Technology and R. J. Rieder and S.

Krishnaswamy of Visidyne, Inc., for **Glenn Research Center.**

Inquiries concerning rights for the commercial use of this invention should be addressed to NASA Glenn Research Center, Commercial Technology Office, Attn: Steve Fedor, Mail Stop 4–8, 21000 Brookpark Road, Cleveland, Ohio 44135. Refer to LEW-16944.

Apparatus for Time- and Wavelength-Resolved Spectroscopy

A pulsed electron gun and a spectrometer are combined.

NASA's Jet Propulsion Laboratory, Pasadena, California

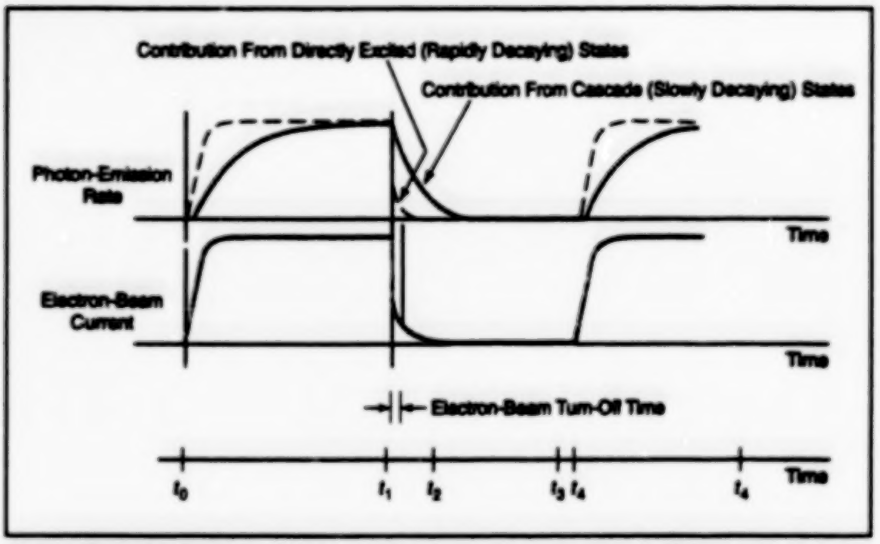

Photon-Emission Rates for directly excited and cascade states decay at different rates when the electron beam is turned off. One can use this difference to discriminate against the faster decay of the directly excited states to obtain the cascade spectrum.

An apparatus that includes a pulsed electron gun and a high-resolution ultraviolet spectrometer has been developed for use in (1) pulsed electron-impact excitation of transitions among the electron-energy states in a gas and (2) measurement of the spectrum of the resulting ultraviolet light emitted by the gas, as a function of wavelength and of time after turn-off of the excitation. The apparatus is designed especially for measuring the Lyman-band emission spectrum of H_2, in order to determine the cascade contribution to this spectrum and thereby to contribute to understanding of cascade contributions to electron-excited spectra of gases in general.

In the electron gun, electrons are generated by a thoriated tungsten filament and electrostatically accelerated through a collimating magnetic field. The electron beam collides at a right angle with a beam of H_2 or another gas of interest effusing through a hole. Light emitted by the electron-excited gas is dispersed by the spectrometer, and the spectrally dispersed photons are detected by use of a channel electron multiplier coated with CsI.

A version of the apparatus as described thus far has been used in prior research to excite and measure spectra in the steady state. The present version of the apparatus is distinguished by its capability for pulsed excitation and time-resolved spectral measurement. In the present version, the basic mode of operation, in which the spectrum is measured as a function of time after turn-off of the excitation, is dictated by the following consideration: Directly excited states that decay to the ground state via resonance transitions typically have lifetimes much shorter than those of cascade states; on the basis of this characteristic, it is possible to discriminate against or suppress contributions of transitions between directly excited resonance states and ground, in order to obtain the desired cascade spectrum.

The electron beam is pulsed on and off (see figure) by applying a rectangular potential waveform to one of the accelerating electrodes in the electron gun. Starting at the beginning of the pulse cycle (time t_0), the electron-beam current increases rapidly from zero to a stable "on" value (typically to ≈200 μA within a time of 150 ns). The gun is maintained in the "on" state for a time sufficient to obtain dynamic equilibrium between excitation and de-excitation processes of the specific excited state that one seeks to analyze. At time t_1, the electron beam is switched off and the electron-beam current falls to zero within ≈30 ns.

After a short gate-delay interval that ends at time t_2, the photon detector in the spectrometer is turned on by use of another rectangular potential waveform. The photon detector is subsequently turned off at t_3, before the beginning of the next pulse cycle at t_4. The gate-delay time ($t_2 - t_1$) can be made long enough that, to a first approximation, the directly excited states can be regarded as having decayed completely to ground. The pulse-repetition period ($t_4 - t_0$), the "beam on" time ($t_1 - t_0$), and the gate-delay time can be varied over a wide range, as needed for analyzing states characterized by effective lifetimes from tens of nanoseconds to ≈8 μs.

This work was done by Joseph Ajello, Dariusz Dziczek, David Hansen, and Geoffrey James of Caltech for **NASA's Jet Propulsion Laboratory.** *Further information is contained in a TSP [see page 1].*

NPO-20809

Shared-Aperture Multiplexed Holographic Scanning Telescopes

Full-aperture scanning would be effected without moving parts.

Goddard Space Flight Center, Greenbelt, Maryland

Shared-aperture multiplexed holographic scanning telescopes have been proposed for use in lidar transceivers and other laser transmitters and receivers in remote sensing instruments. Examples of instruments that could incorporate the proposed telescopes include airborne terrain mappers, and lidar wind-sheer-profiling systems to increase safety of airplane takeoffs and landings. Unlike prior scanning telescopes, the proposed telescopes would contain no moving parts; hence,

relative to prior scanning telescopes, the proposed telescopes could be made lighter, more compact, and more reliable.

Instead of conventional reflective or refractive optics, shared-aperture multiplexed holographic scanning telescopes would utilize diffractive optics in the form of holographic optical elements (HOEs). A telescope of this type is said to be shared-aperture multiplexed (SAM) because a number of HOEs would be multiplexed into a single film, the area of which would define a single, shared aperture. Each HOE in the film would be optically addressable by virtue of its angular selectivity, which would define a field of view (FOV) centered on a line of sight different from the lines of sight of the other HOEs. Thus, by optically addressing the various HOEs in sequence, one could aim the telescope sequentially along different lines of sight.

In addition to separate FOVs, the HOEs in the film would have separate field stops, for example, located at various angles around a circle (see figure). Each HOE would be optically addressed by transmitting a laser beam through the HOE along the appropriate line of sight, which would appear to emanate from one of the field stops. This could be accomplished by use of a separate laser for each line of sight. Alternatively, one could steer a single laser beam sequentially through virtual field stops, either by diffractive beam steering mechanisms, or mini-mechanical scanner, or even microelectromechanical systems (MEMS) technology.

In an alternative optical configuration, the central portion of the SAM optic would be used for transmitting only. In this case, the focal spots from which the laser beam would appear to emanate would be offset from the receiver foci and the central transmitting portion of the SAM optic would no longer be available for receiving. Moreover, in this case, there would be an option to superimpose the receiving foci so that a single detector could be used for all FOVs, provided that the transmitted laser pulses were sufficiently separated in time that lidar return signals would not overlap.

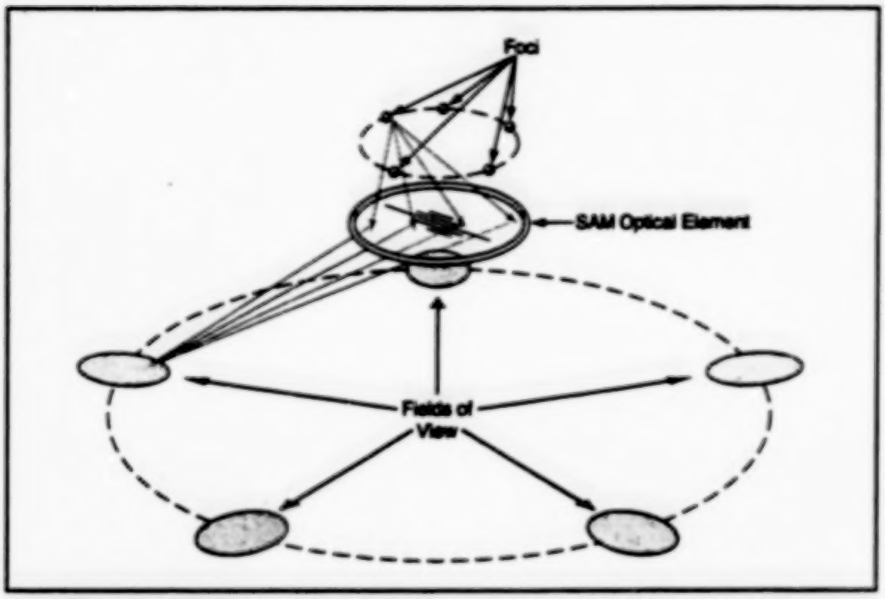

The SAM Optical Element would be a single film containing multiple HOEs, each of which would provide a unique field of view and focus.

It is worth emphasizing that the proposed telescopes would scan in a step-and-stare mode rather than in the continuous mode of mechanical scanning. Although this may seem at first glance to be disadvantageous, it may not be; indeed, it could even be advantageous. In particular, there is some agreement within the Doppler lidar community that continuous scanning is not needed, and that a step-and-stare approach to gathering data from different look angles may be preferred because it would eliminate the need for lag-angle compensation. (In a mechanically scanned lidar system, the lag angle is a consequence of rotation of a scanner during the time it takes a light pulse from the laser transmitter to travel to the target and back.)

This work was done by Geary Karl Schwemmer of **Goddard Space Flight Center** *and Richard Rallison of Raicon, Inc. Further information is contained in a TSP [see page 1].*

This invention is owned by NASA, and a patent application has been filed. Inquiries concerning nonexclusive or exclusive license for its commercial development should be addressed to the Patent Counsel, Goddard Space Flight Center [see page 1]. Refer to GSC-14240.

Books and Reports

Capture and Escape of Charge Carriers in Quantum Dots

A report describes an experimental investigation of effects of thermally induced intermixing of $In_{0.6}Ga_{0.4}As$ and GaAs on the dynamics of photoexcited charge carriers in $In_{0.6}Ga_{0.4}As$/GaAs quantum dots. The quantum dots (nanometer-size islands of $In_{0.6}Ga_{0.4}As$ surrounded by GaAs) were grown by metal-organic chemical-vapor deposition. The dynamics at temperatures from 60 to 300 K were investigated by time-resolved photoluminescence measurements with subpicosecond temporal resolution, on both specimens as grown and specimens in which intermixing had been effected by a post-growth anneal. The measurement data were interpreted as signifying that at lower temperatures, the carrier lifetimes in the dots are determined by radiative recombination, which becomes substantially faster after intermixing, while at temperatures >150 K, thermal emission of carriers predominates. Capture of carriers into the dots was found to be fast and governed by carrier-carrier scattering; at room temperature and high excitation intensity, a carrier capture time of 0.72 ps was observed in the intermixed dots. These findings have implications for the development of quantum-dot lasers.

This work was done by Rosa Leon of Caltech for **NASA's Jet Propulsion Laboratory**. *To obtain a copy of the report, "Carrier capture and escape in $In_xGa_{1-x}As$/GaAs quantum dots: Effects of intermixing," see TSP's [page 1].*
NPO-20766

Rayleigh-Scattering Measurements in Underexpanded Jets

A report describes experiments in which time-averaged and unsteady local variations in the densities of underexpanded supersonic free jets issuing from a choked circular nozzle were measured by laser-induced Rayleigh scattering. This study is part of a continuing effort to understand the generation of screech noise by supersonic jets. The Rayleigh scattering technique used dust-free air for primary and entrained flows, a continuous wave laser, and photon counting electronics for reliable and accurate measurement. Time-averaged radial density profiles obtained at various axial stations ranging to 10 jet diameters downstream show the development of a jet shear layer and the decay of shock cells. Data on unsteady density variations show the evolution of large turbulent vortices modulated periodically along the flow direction. Comparison of data from these measurements with data from previous measurements revealed the following: The periodic modulation in density and convective velocity of turbulent vortices coincides with the modulation of pressure fluctuations outside the flow boundary. The spatial periodicity of modulation is different from the shock spacing and is associated, instead, with a standing wave. The standing wave is formed between downstream-moving turbulent vortices and the upstream-propagating screech sound waves. It extends from inside the shear layer to the near-field outside the flow. All of these indicate that the sound sources are located a standing wavelength apart.

This work was done by J. Panda of Modern Technologies Corp. and R. G. Seasholtz of **Glenn Research Center**. *To obtain a copy of the report, "Measurement of shock structure and shock-vortex interaction in underexpanded jets using Rayleigh scattering," see TSP's [page 1].*

Inquiries concerning rights for the commercial use of this invention should be addressed to NASA Glenn Research Center, Commercial Technology Office, Attn: Steve Fedor, Mail Stop 4–8, 21000 Brookpark Road, Cleveland, Ohio 44135. Refer to LEW-17119.

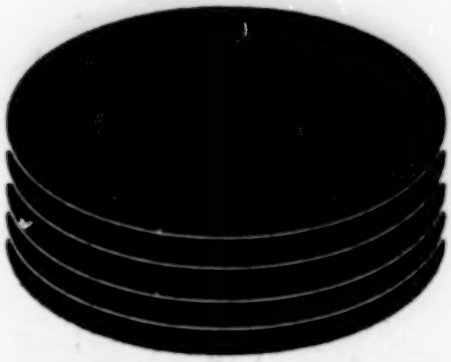

Computer Programs

Electronic Systems

25 Program Tracks Operation of a Remote Solid-State Recorder

Physical Sciences

25 Computing Radiation Fluxes, Power, and Temperature for TOPEX

25 Program for Updating Parameters of Thermal Models

Mathematics and Information Sciences

25 Library for Developing Spacecraft-Mission-Planning Software

26 Software for Real-Time Transfer of GPS Data Over the Open Internet

BLANK PAGE

Electronic Systems

Program Tracks Operation of a Remote Solid-State Recorder

Solid State Recorder Pointer Tracker (SSRPT) is a computer program developed specifically to aid ground-based monitoring and control of two redundant solid-state recorders (SSRs) aboard the Cassini Spacecraft. The SSRs store telemetry data until downlink times, which are limited to a total of about 8 hours per week. With respect to the SSRs, SSRPT serves as an inexpensive substitute for a complete hardware-and-software simulator of the spacecraft. SSRPT makes it possible to track recording- and playback-pointer address positions in the SSR, thereby making it possible to (1) minimize the use of precious uplink and downlink time by commanding the downlinking of only data of interest stored at known addresses and (2) inhibiting recording at addresses from which data are required but have not yet been played back. SSRPT functions in two modes: (1) a calculator mode, in which it performs basic computations where recording and playback bit rates are multiplied by time intervals; and (2) a sequence-predictor mode, in which it predicts pointer positions according to the time line of commands sent to the spacecraft.

This work was done by Edwin P. Kan, Shahan Petrosian, and Barbara Larson of Caltech for **NASA's Jet Propulsion Laboratory**. *Further information is contained in a TSP [see page 1].*

This software is available for commercial licensing. Please contact Don Hart of the California Institute of Technology at (818) 393-3425. Refer to NPO-20423.

Physical Sciences

Computing Radiation Fluxes, Power, and Temperature for TOPEX

A computer program performs a unified analysis of the radiation exposure, the temperatures, and the power generation and distribution for predicting the performance of the TOPEX satellite on orbit and during maneuvers. The unified analysis is needed because all aspects are interdependent. The power-generating capacity of the solar array of the satellite depends on both the impinging radiation fluxes and the temperatures of the panels. The temperatures, in turn, depend on the power output of the array in addition to the radiation fluxes. Only by considering electric-power generation and consumption, radiation fluxes, and temperatures together can one predict any one of them as well as the state of charge, the voltage, and the current of the batteries. The present computer program predicts the power profile and the solar, albedo, and infrared fluxes on all surfaces of the satellite. It calculates the temperatures of the solar array and its power-generating capacity as function of radiation exposure and temperature. Battery currents and voltages are determined on the basis of the calculated state of charge of the batteries and the power-generating capacity of the solar array as a function of its radiation exposure and its temperatures. All pertinent values are stored in files with any desired time interval.

This program was written by Robert Richter of Caltech for **NASA's Jet Propulsion Laboratory**. *Further information is contained in a TSP [see page 1].*

This software is available for commercial licensing. Please contact Don Hart of the California Institute of Technology at (818) 393-3425. Refer to NPO-21018.

Program for Updating Parameters of Thermal Models

Parameter Identification in Thermal Networks (PITN) is a computer program developed to satisfy a need to update parameters in mathematical models of thermal systems in order to make the temperatures computed by the models equal to the temperatures measured in tests of the corresponding real systems. PITN is suitable for application to network-type models of scientific instruments and general engineering systems, including telescopes, spectrometers, and spacecraft. Relative to software developed previously for the same purpose, PITN can readily be applied to more complex models and yields results in less time. In addition, PITN can accommodate nonlinearities in thermal models (nonlinearities are typically associated with radiative heat transfer). PITN is based partly on the formulation of the parameter-matching problem as a nonlinear least-squares optimization problem, which can be solved by use of very fast and robust optimization techniques. The speed and accuracy of computations are increased by use of analytic expressions for temperature differentials.

This program was written by Miltiadis Papalexandris and Mark Milman of Caltech for **NASA's Jet Propulsion Laboratory**. *Further information is contained in a TSP [see page 1].*

This software is available for commercial licensing. Please contact Don Hart of the California Institute of Technology at (818) 393-3425. Refer to NPO-21067.

Mathematics and Information Sciences

Library for Developing Spacecraft-Mission-Planning Software

The Platform Independent Software Components for the Exploration of Space (PISCES) software library provides for web-based, collaborative development of computer programs for planning trajectories and other trajectory-related aspects of spacecraft-mission design. The PISCES library was built using state-of-the-art object-oriented concepts and software-development methodologies. The components of PISCES include Java-language application programs that implement trajectory-propagation algorithms, including gravity models, atmosphere models, planetary ephemerides, and orbital propagation. Extensive generalized rendezvous-planning software is also included. These components are arranged in a hierarchy of classes that facilitates the re-use of the components in planning trajectories. As its full name suggests, the first advantage of the PISCES library is platform-independence. By using the "write once, run anywhere" capability of Java, anyone can use the classes and application programs with a Java virtual machine, which is available in most web-browser programs. The second advantage of the library is expandability. Object orientation facilitates the expansion of the library through the simple creation of a new class.

This work was done by Don Pearson and Dustin Hamm of **Johnson Space Center**, *with support from Jonathan K. Weaver of JSC and Brad Holcomb and Brian Kubena of Lockheed Martin. Further information is contained in a TSP [see page 1].*

MSC-22983

Software for Real-Time Transfer of GPS Data Over the Open Internet

Real-Time Net Transfer (RTNT) software allows for efficient and reliable transport of raw, GPS (Global Positioning System) observables over the open Internet. Efficiency is achieved by editing and compressing the GPS observables at the remote site, and by using User Datagram Protocol (UDP) rather than the higher overhead required of Transmission Control Protocol (TCP). However, TCP reliability is still achieved by the central server (the central collection computer) by monitoring sequence numbers of the remote client's packets. If there is a skip in sequence numbers, the central server may request retransmission of missed data packets from the remote clients. In this way over 98 percent of the data is returned to the central server. Once the central server receives the data, it may additionally retransmit the packets to other servers on the open Internet. This provides the capability of merging regional servers into a global server. There is a particular secondary server also running receiving data packets from the primary global server. If the secondary server no longer sees incoming packets, it will reroute the entire global network to itself. This provides a backup system should the primary server fail.

RTNT returns data from geodetic-quality receivers, such as Ashtech Z-12s, Turbo-Rogues, and AOA Benchmark receivers. Module construction of the s/w processes permits addition of other receivers. Five of six basic GPS observables are compressed down to 14.5 bytes per 1 Hz epoch, per GPS s/c tracked. The two phase observables (L1,L2) have a resolution of 0.02 mm, and the three range observables (CA,P1,P2) have a resolution of 1 mm.

RTNT is currently returning data with a latency of less than two seconds from a global network of 17 receivers. Latency here is defined as the time tag of the GPS observable and the time that the packet arrives at the central server. The web page, *http://gipsy.jpl.nasa.gov/igdg/demo/index.html* contains the real-time operating status of the RTNT's global network. Data latencies and the number of GPS spacecraft tracked per remote site for the previous hour can be monitored through this web page.

Once the data arrives at the central server, it is sorted by epoch, duplicate packets are rejected, request for retransmission of missed data packets are made, and the data is placed into a revolving segment of shared memory. From there, JPL's Real-Time Gipsy (RTG) software is used to compute global differential corrections to the GPS broadcast orbits and broadcast clocks. Real-time user position accuracy from this global differential system is 8 cm (RMS) in horizontal, and 20 cm (RMS) in vertical. The above web page also contains a live demo of the receiver at JPL demonstrating these accuracies.

RTNT also provides the mechanism to distribute both the GPS broadcast orbits and clocks, and RTG's global differential corrections to the broadcast orbits and clocks over the open Internet. A server will fork dedicated TCP processes to any client making requests.

This program was written by Ronald Muellerschoen of Caltech for **NASA's Jet Propulsion Laboratory**. *Further information is contained in a TSP [see page 1].*

This software is available for commercial licensing. Please contact Don Hart of the California Institute of Technology at (818) 393-3425. Refer to NPO-20976.

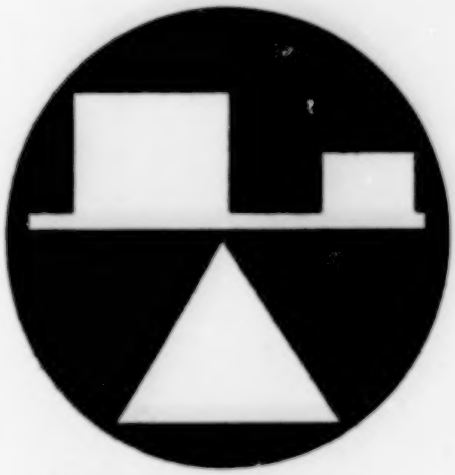

Mechanics

Hardware, Techniques, and Processes

29 Lightweight, Collapsible Hyperbaric Chamber With Airlock

BLANK PAGE

Lightweight, Collapsible Hyperbaric Chamber With Airlock

Hyperbaric treatment could be provided in settings remote from major medical facilities.

Lyndon B. Johnson Space Center, Houston, Texas

A lightweight, collapsible hyperbaric-chamber/airlock system has been proposed as a portable unit for treating decompression sickness. Copies of the system could be stowed compactly and deployed when needed in settings in which decompression sickness is expected to occur occasionally but in which conventional heavy, rigid hyperbaric chambers are not available. Such settings include aviation, submarine operations, diving, and spaceflight.

The system (see figure) would include a main hyperbaric chamber and an integral airlock, both capable of maintaining an interior pressure of 2 atm (0.2 MPa) for one patient and a medical attendant. One would gain access to the main hyperbaric chamber via the hatches at the ends of the airlock. The central hatch ring at the junction of the airlock and the main chamber would be penetrated by hermetically sealed conduits that would provide air, medical oxygen, electrical power, and communication from external equipment to both the airlock and the main chamber.

The walls of the main chamber and the airlock would be made of multiple layers of lightweight, flexible materials, and could be folded to a small volume. Included among the wall layers would be pressure bladders, plus flexible circumferential and longitudinal straps that would afford the strength to withstand pressurization. The airlock hatch ring would be sized to fit within the central hatch ring to minimize storage volume. An internal skeleton of interconnected low-pressure inflatable toroids (reminiscent of an inflatable raft) would maintain the main chamber and airlock in the expanded condition when the main chamber, the airlock, or both were not pressurized, thereby facilitating entry and egress. The inflatable toroids could also serve as a cushion for the patient during hyperbaric treatment.

The central and airlock hatch rings would serve as seal lands for the central and airlock hatches. The hatches would include rings, to which would be attached strap and pressure-bladder layers like those of the chamber walls. The hatches would be elliptical so that they (rotated 90°) could fit through the elliptical hatch openings to facilitate access. The hatches would be held in place temporarily by magnets until pressurization seated them firmly and compressed the hatch seals.

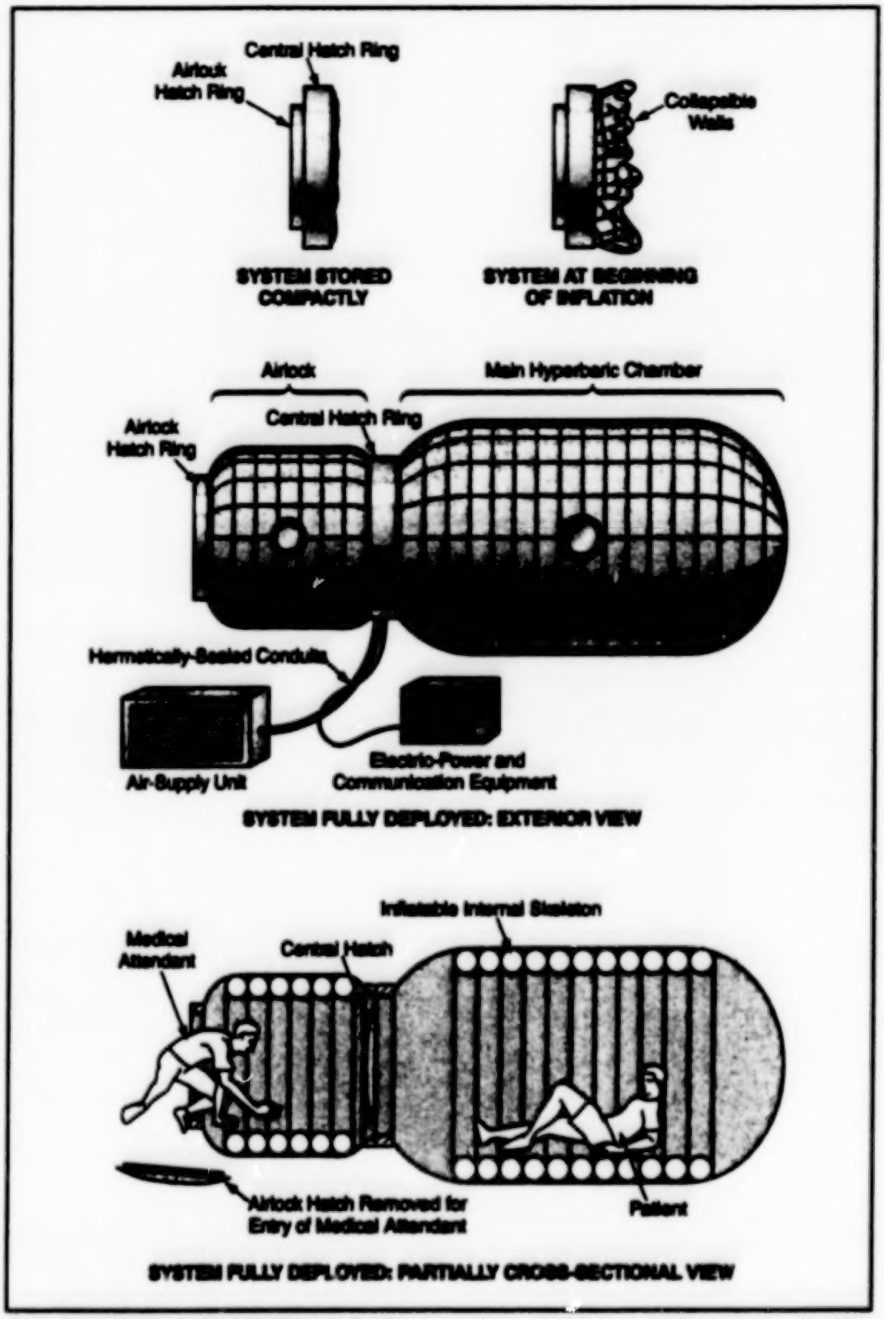

This Hyperbaric Chamber/Airlock System could be stored in a small volume, yet when deployed, it would accommodate a patient and a medical attendant.

This work was done by William C. Schneider, James P. Locke, and Horacio M. De La Fuente of Johnson Space Center. Further information is contained in a TSP [see page 1].

This invention is owned by NASA, and a patent application has been filed. Inquiries concerning nonexclusive or exclusive license for its commercial development should be addressed to the Patent Counsel, Johnson Space Center, (281) 483-0837. Refer to MSC-23076.

Machinery

Hardware, Techniques, and Processes

33 Reconfigurable Exploratory Robotic Vehicles

Reconfigurable Exploratory Robotic Vehicles

Instrumentation and mobility units could be concatenated as needed.

NASA's Jet Propulsion Laboratory, Pasadena, California

A family of rugged, modular, reconfigurable, instrumented robotic vehicles has been proposed for use in exploration of the surfaces of Mars and other remote planets. These or similar vehicles could also be useful in such diverse terrestrial applications as exploration of volcanic craters or other hostile terrain, military reconnaissance, inspection of hazardous sites, or searching for victims of earthquakes, landslides, or avalanches. There might even be a market for simplified versions of these vehicles as toys.

The proposed vehicles are denoted generally by the term *Axeln*, where n is an even number equal to the number of main wheels. The simplest vehicle of this type would be an *Axel2* — a two-main-wheel module that would superficially resemble the rear axle plus rear wheels of an automobile (see Figure 1). In addition to the two main wheels, an *Axel2* would include a caster wheel (or flat surfboard) attached to the axle by an actuated caster link. The motion (about three quarters of a circle) of the caster link would be used to control the rotation of the axle in order to tilt, to the desired angle, any sensors that might be mounted on the axle. The *Axel2* would hence use the same sensors for forward and backward driving. In the vertical position, the caster link is used as an antenna for wireless communication. Two brushes attached to either side of the caster link wipe dust off the solar cells.

In addition to the sensors, the axle of an *Axel2* would house computer modules and three motors and associated mechanisms for driving the main wheels and the caster link. Solar cells would be mounted on the outside of the axle except at a mid-length portion, where an assembly containing the caster-link actuator and two module interfaces (one at each end) would be located. Rechargeable batteries would be placed inside the wheel hubs.

One would construct an *Axeln* ($n > 2$) as an assembly of multiple *Axel2*'s plus one or more instrument module(s) connected to each other at the module interfaces (see Figure 2). The module interfaces would contain standardized electrical and mechanical connections, including spring-loaded universal joints, about which the modules could comply to adapt to the terrain. Data would be communicated between modules via fast serial links.

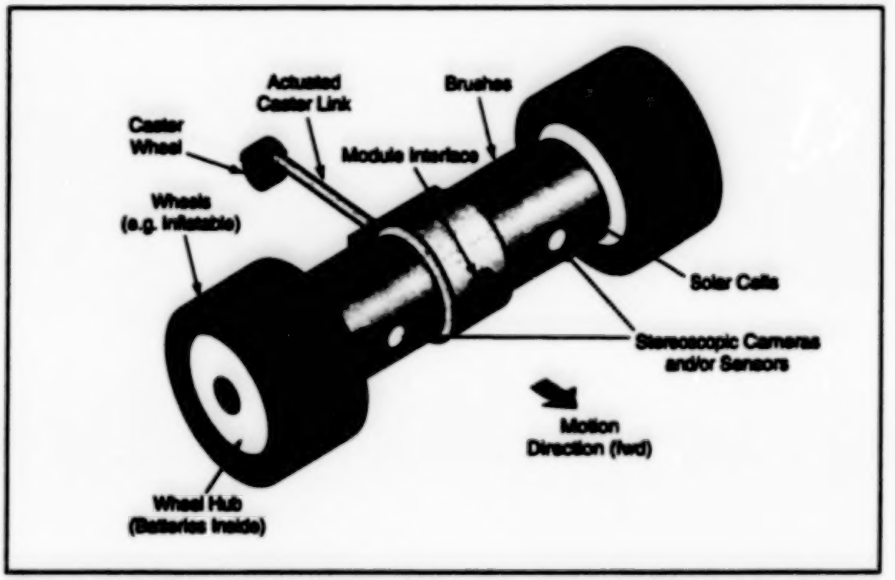

Figure 1. An *Axel2* would be the simplest vehicle module, used as a building block for vehicles of greater complexity.

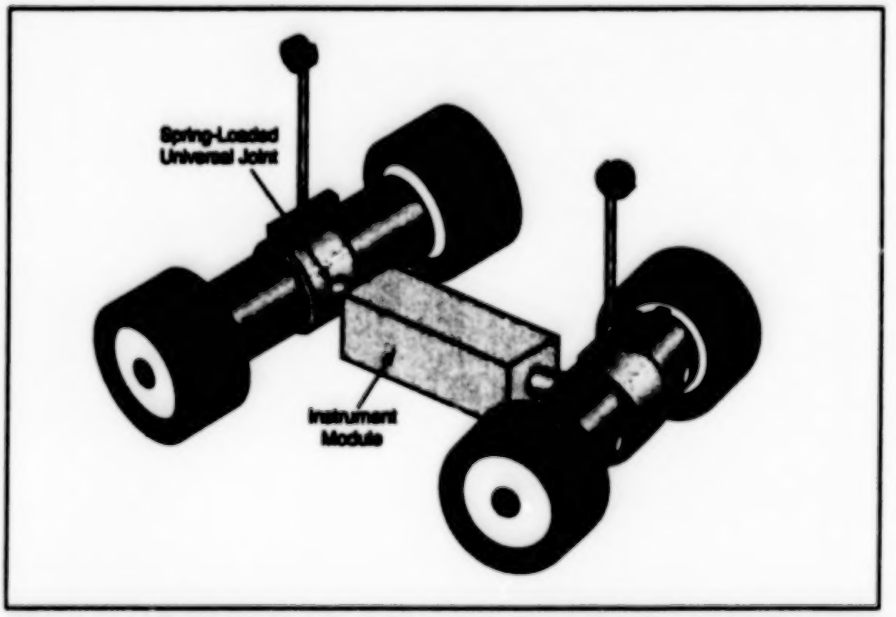

Figure 2. An *Axel4* would consist of two *Axel2*s connected to opposite ends of an instrument module.

An *Axeln* would amount to a train carrying $n/2 - 1$ instrument modules. The instrument modules would contain additional computational units that, in addition to processing of instrument readings, could contribute to coordination of train motion. In other words, the "intelligence" of an *Axeln*, and thus the sophistication of the maneuvers that it could perform, would increase with n.

The symmetrical design of the modules would enable them to operate in any stable orientation, including upside-down; this feature would contribute to robustness of operation in rough terrain, including the ability to recover after falling off a cliff (in the case of *Axeln* where $n < 6$). The simple and modular design of the *Axels* provides better maneuverability using fewer actuators and sensors and hence lower power requirements than traditional rovers. The

system features scalable complexity: the motion control algorithms for the *Axel2* are very simple; and as the size of the *Axel* train grows, the complexity of the algorithms increases.

The proposed vehicles would be designed to diagnose themselves to detect nonfunctional modules. They would be programmed to travel to robotic service depots, called assembly stations, where nonfunctional modules would be disconnected and replaced by functional ones.

This work was done by Issa Nesnas of Caltech for **NASA's Jet Propulsion Laboratory**. *Further information is contained in a TSP [see page 1].*
NPO-20944

Mathematics and Information Sciences

Hardware, Techniques, and Processes

37 Common Database Interface and Report Generator

37 Software for Secure Distribution of Data

38 Coherent Phase Line Enhancer: a Method of Spectral Analysis

BLANK PAGE

Common Database Interface and Report Generator

This program yields reusable, centralized code.

Lyndon B. Johnson Space Center, Houston, Texas

The Common Database Interface and Report Generator is a computer program that serves as both (1) a single common interface for data-base application programs to gain access to local or remote data bases by use of Structured Query Language (SQL) operators and (2) a report generator.

The data-base-interface portion of the program enables a calling program to gain access to an Oracle data base by use of all of the basic SQL operators (SELECT, INSERT, UPDATE, DELETE, COMMIT, and ROLLBACK). The program provides capabilities for logging in, logging out, and reporting errors. Each data-base function corresponds to a function callable in the C computing language. The calling data-base function passes the SQL statement as an argument to the called function.

For the SELECT function, the calling function also passes the function-specific callback routine as an argument. The callback routine is executed after each record has been retrieved from the data base. This unique approach allows the SELECT function without buffering of all the retrieved data. Status information is returned in the function return value.

The report-generator part of the program produces a plain text report, based on the contents of a report template. Instead of writing individual functions for each report, the user need only write templates to direct the report generator to generate the report. Any changes in the format of a report can be made by modifying the report template; there is no need to modify any computer code.

The report-generator part of the program invokes a report-template-parser subprogram to read in the report template via a report-template scanner. Then the report-generator part of the program passes, to a reporting-engine subprogram, the report structure and the arguments passed in from the calling program. The reporting engine generates the report output, invoking a data-base-access module to obtain data for the report and invoking a page-construction module to format the output.

The program affords full-featured error reporting capabilities. Multiple tables can be updated from the computer display screen; this feature saves a significant number of hours. Report templates can easily be changed without stopping the program; this feature helps to reduce cost.

The primary benefits afforded by this program are that (1) it yields reusable computer code, thereby reducing the cost of developing and maintaining code, reducing the number of lines of code that must be maintained, and (2) it centralizes the code, thereby making it easy to maintain. Because there is no need for a programmer to write Pro*C code, the level of required programming skill is correspondingly reduced.

This work was done by Fran Y. Mi of United Space Alliance and Kevin N. Shaum of Unisys for **Johnson Space Center**. *Further information is contained in a TSP [see page 1].*
MSC-22819

Software for Secure Distribution of Data

Many users at remote locations can work on the same set of data.

NASA's Jet Propulsion Laboratory, Pasadena, California

MECS is a computer program for the automated, secure, rapid, and efficient transfer of data between a central source and users at multiple distant locations. "MECS" signifies "Multi-mission Encrypted Communication System." MECS enables many users to collaborate securely on a shared plan or set of data.

MECS was part of the Mars polar lander mission operations environment, and enabled for the first time in NASA's history, distributed operations over the Internet during a mission operational readiness test. It has allowed remote scientists to lead field tests of the FIDO rover, which is the prototype for the Mars '03 rover.

MECS transfers data from a mission control center to remote users, and from the remote users back to the mission control center. MECS is designed to work with previously developed mission application programs that, in their original forms, do not support secure distributed operation; MECS can often enable secure distributed operation with little or no modification of the previously developed application programs. MECS operates in such a way as to be transparent to a remote user. Files simply appear on the remote user's computer as they become available, and files are transmitted back to a server computer at the mission control center when the user saves them in specific directories.

All MECS connections are authenticated by use of the NASA public key infrastructure, and all communications are encrypted by use of the Secure Sockets Layer (SSL) protocol. It is nearly impossible to decipher intercepted data that have been transmitted via MECS, and in order to defeat the authentication protocol, it would be necessary to compromise the NASA Ames Certificate Authority, which is highly protected. A copy of the MECS client software cannot be activated unless the remote user to whom the copy has been assigned presents a personal security profile that is kept on a floppy disk in the possession of the user. To obtain a security profile, a remote user must appear in person and provide positive identification at a security office at a NASA center. The NASA public key infrastructure handles the periodic updating of users' security profiles and protects the central certificate authority.

MECS is implemented as two Java programs. For each mission, there is typically one server program operating on a computer behind the mission firewall, and many client programs, each running on a remote user's computer. The MECS administrator indicates which files should be received by the remote users, and the MECS clients automatically download the data as it becomes available. All data is compressed and encrypted while in transit, and is automatically decompressed and moved to the proper locations on the client's computer.

Each remote user starts the MECS client program and specifies the address of the MECS server. The MECS client and server programs authenticate each other, and then the client program transmits the current state of the remote user's data base to the server. The server then transmits all of the files necessary to bring the remote user's data base up to date. Periodically, the MECS client program automatically

communicates with the server to determine whether new data have arrived.

In its original form, MECS can be used to implement secure on-line discussions, shared workspaces, and collaborative generation of command sequences. There are also potential commercial applications for suitably modified versions of MECS: Many organizations need an efficient means of secure synchronization of remote systems. Inasmuch as nearly every software system developed previously to satisfy this need requires that the client initiate a request for specified data, there is no guarantee that a client has received the latest update to the shared data; in contrast, MECS, keeps client data files up to date.

This work was done by Paul Backes and Jeffrey Norris of Caltech for **NASA's Jet Propulsion Laboratory**. *Further information is contained in a TSP [see page 1].*

In accordance with Public Law 96-517, the contractor has elected to retain title to this invention. Inquiries concerning rights for its commercial use should be addressed to

Technology Reporting Office
JPL
Mail Stop 249-103
4800 Oak Grove Drive
Pasadena, CA 91109
(818) 354-2240

Refer to NPO-20844, volume and number of this NASA Tech Briefs *issue, and the page number.*

Coherent Phase Line Enhancer: a Method of Spectral Analysis

This method enables detection of weak signals that would otherwise be masked by noise.

Marshall Space Flight Center, Alabama

The term "coherent phase line enhancer" (CPLE) refers to a dual-transform method of spectral analysis that enhances the detection of periodic and quasi-periodic signals buried in wide-band noise. The CPLE is particularly useful for increasing the signal-to-noise ratios of spectral peaks ("lines") that represent periodic and quasi-periodic components of measurements of vibration, dynamic strain, and/or dynamic pressure in a turbine or other rotating machine. The purpose of such measurements, spectral analysis, and enhancement of spectral peaks is to assess machine performance and identify spectral signatures of bearing or gear-train defects.

Other machine-diagnostic spectral-analysis methods related to the CPLE have been described in several prior articles in *NASA Tech Briefs*. The need for the CPLE and those other methods arises, in part, because in conventional spectral displays, peak patterns are frequently difficult to assess in cases in which peaks are at or below the amplitude of wide-band noise. ["Conventional spectral displays" as used here denotes those produced by fast-Fourier-transform (FFT) processing of digitized signals.] In such displays, periodic signals may not be separated from wide-band noise because the phase information needed to show the peaks for these signals is missing after FFT processing. The CPLE involves a second transformation that restores the needed phase information. In addition, in the CPLE, the discreteness of each spectral component is quantified by a bandwidth coherence value.

The traditional method of estimating the auto power spectral density (PSD) function involves ensemble processing of the FFT amplitude of each segmented data block and discarding the FFT phase information. The resulting "ensemble amplitude averaging" PSD function is widely used in many commercial test and measurement products. For the purpose of separating a periodic signal from noise, additional signal-enhancement capability can be achieved by including phase-correlated information in the ensemble processing. After the original signal is transformed from the time domain to the frequency domain, the spectral record consists of an ensemble of blocks. In the CPLE, a second transform converts each spectral component along the ensemble direction into an "equivalent" wave-number domain, in which signal components are enhanced by virtue of their coherent phase relationships among the ensemble segments.

In comparison with spectrum obtained by FFT processing only, a CPLE spectrum provides a more accurate estimate of the frequency of a periodic signal. Moreover, the difference between the coherent phase characteristic of a periodic signal and the random phase of wide-band noise is more apparent in the wave-number domain. As a result, in comparison with a conventional power spectrum, a CPLE spectrum enables better detection of periodic signals. Unlike some other filtering techniques (e.g., adaptive filter, adaptive line enhancer, and the like) used to enhance signals, the CPLE can be the basis of a relatively simple and stable approach that can be easily implemented in the frequency domain along with the FFT.

The quasi-periodicity (as distinguished from pure periodicity) of the vibration signal from a typical rotating machine poses a major obstacle to the direct application of the CPLE to analysis of these signals. The rotation-speed-related components of the signal (e.g., synchronous harmonics and subharmonics, bearing signatures, gear signatures, and the like) are all quasi-periodic because rotation tends to momentarily accelerate or decelerate as the load on the machine varies. A direct application of the CPLE to the signal does not provide any enhancement because only weak (if any) coherent phase relationships exist among the ensemble segments. However, one can obtain the desired enhancement by following either or both of the following two approaches:

The first approach is called "CPLE/OT" (where "OT" signifies "Order Tracking method"). This method requires an additional pulse tachometer (key-phasor) signal. Measurement of the time between the pulses yields an instantaneous value of the rotation period once per revolution. On the basis of this measurement, the original digital signal, which is sampled at uniform intervals of time, is then resampled with a fixed number of samples during each revolution. The resampling involves the use of either linear interpolation or (in the case of large variations of speed) spline-curve-fit interpolation. The resampling is utilized in the conventional synchronous timer averaging (STA) method. STA enhances a waveform through direct time averaging of the resampled waveform over many revolutions. Within the resampled signal, all the speed-related components are periodic. Therefore, CPLE spectral analysis is applicable to speed-related signal enhancement.

The second approach is called "CPLE/PSEM" (where "PSEM" denotes "phase synchronized enhancement method"). This method does not require the key-phasor signal. The PSEM involves a phase-to-time conversion algorithm that transforms the instantaneous phase of a reference component of the signal into the desired resampling time for synchronization. (The reference component is selected by the user and is typically synchronous with

either the rotation or a harmonic thereof.) Within the resulting PSBM signal, both the reference component and all its coherently correlated components become periodic. Consequently, when CPLE spectral analysis is applied to the PSBM signal, enhanced results are obtained.

This work was done by Jen-Yi Jong of AI Signal Research, Inc., for **Marshall Space Flight Center**. *For further information, please contact the company at* **www.aisignal.com** *or (256) 551-0008.*

Inquiries concerning rights for the commercial use of this invention should be addressed to the Patent Counsel, Marshall Space Flight Center [see page 1]. Refer to MFS-31426.

BLANK PAGE

Life Sciences

Hardware, Techniques, and Processes

43 Engineered Bioremediation of Contaminated Soil

44 Microgravity Tissue Engineering

BLANK PAGE

Engineered Bioremediation of Contaminated Soil

Electrokinetic transport is utilized to enhance biodegradation of contaminants by micro-organisms.

John F. Kennedy Space Center, Florida

Electrokinetically enhanced bioremediation (EEB) is a method of engineered bioremediation of soil contaminated by such organic compounds as solvents and petroleum products. As depicted schematically in the figure, EEB involves the utilization of controlled flows of liquids and gases into and out of the ground via wells, in conjunction with electrokinetic transport of matter through pores in the soil, to provide reagents and nutrients that enhance the natural degradation of contaminants by indigenous and/or introduced micro-organisms.

The operational parameters of an EEB setup can be tailored to obtain the desired flows of reagents and nutrients in variably textured and layered soils of variable hydraulic permeability and of moisture content that can range from saturation down to as little as about 7 percent. A major attractive feature of EEB is the ability to control the movements of charged anionic and cationic as well as non-charged chemical species.

The basic components of electrokinetic enhancement of bioremediation are the following:

- Ions are transported by electromigration; that is, with minimum transport of liquid through the soil. The ions of interest include nutrient agents, electron donors (e.g., lactate) or electron acceptors (e.g., nitrate or sulfate) added to the soil. Electromigration is utilized as an efficient mode of electrokinetic transport in vadose-zone soils.
- Water in soil is pumped (horizontally or vertically, depending on the positions of electrode wells) by induced electro-osmotic flow. Whereas the hydraulic flow used in older methods decreases with decreasing pore size and is thus not effective for treating tightly packed soil, electro-osmotic flow is less restricted by tight packing. Electro-osmosis is utilized to enhance the transport of both ions and such noncharged particles as micro-organisms, by moving water from anodes (positive electrodes) toward cathodes (negative electrodes).
- Electrophoresis induced in soil under an applied electric field is used to control the transport and/or distribution of micro-organisms throughout the treated soil volume. The beneficial effect of electrophoresis can be augmented or otherwise modified by use of electro-osmotic flushing of the soil.
- The applied electric current can be utilized to heat the soil to the optimum temperature for bioremediation.
- The gaseous and liquid products of electrolysis of water in the soil are removed from electrode wells and mixed and reinjected into the ground as needed to maintain the pH of the soil within a range favorable for bioremediation.

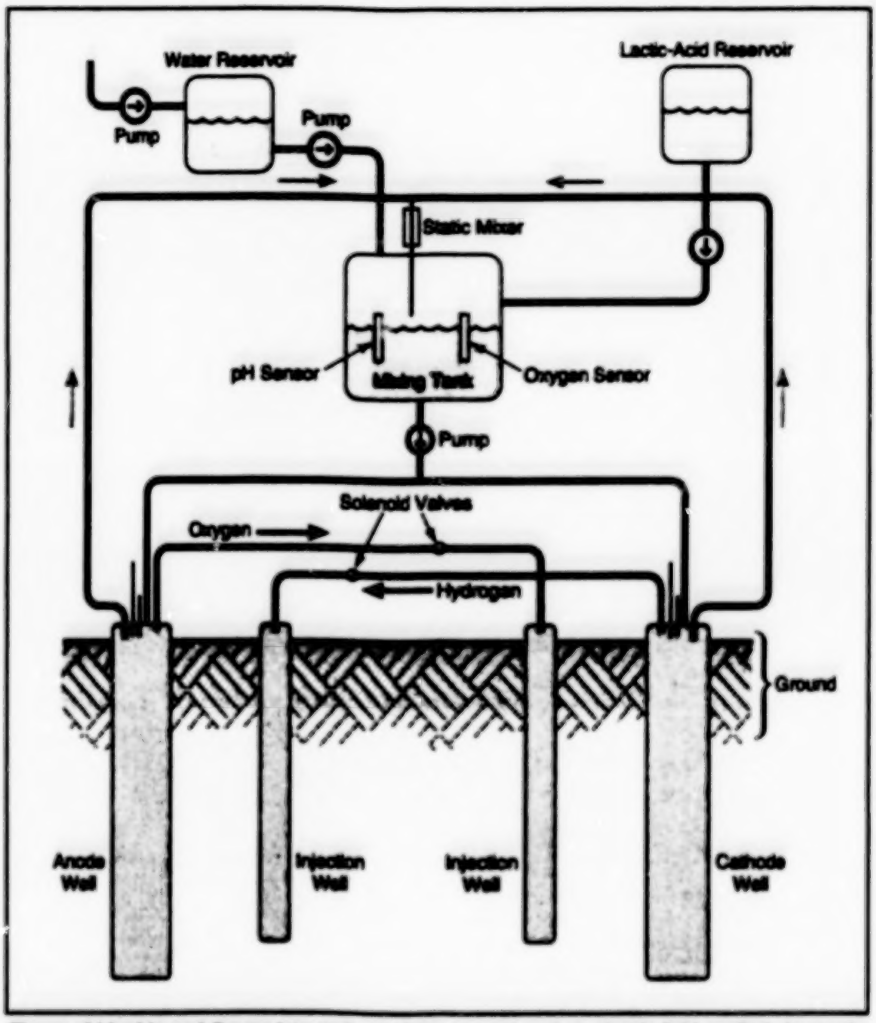

Flows of Liquids and Gases into and out of the ground and an electric field applied via anode and cathode wells are all controlled by a computer in response to sensed conditions and according to a schedule to generate conditions that favor *in situ* bioremediation of the soil.

This work was done by Dalbor Hodko, G. Duncan Hitchens, Tom D. Rogers, James W. Magnuson, and Jeffrey K. Dillon of Lynntech, Inc., for Kennedy Space Center. Further information is contained in a TSP [see page 1].

In accordance with Public Law 96-517, the contractor has elected to retain title to this invention. Inquiries concerning rights for its commercial use should be addressed to

Lynntech, Inc.
7610 Eastman Drive, Suite 105
College Station, TX 77840

Refer to KSC-12045, volume and number of this NASA Tech Briefs *issue, and the page number.*

Microgravity Tissue Engineering

Cartilage and cardiac muscle can be engineered for research in normal gravity and microgravity.

Lyndon B. Johnson Space Center, Houston, Texas

A continuing program of research and development focuses on engineering of functional cartilage and cardiac muscle for scientific research and for eventual use in transplants. The program involves the use of cells, polymer scaffolds, and bioreactor vessels. A polymer scaffold serves as a three-dimensional structure to which cells can attach. Once attached, the cells can regenerate full tissues, and then the polymer scaffold becomes biodegraded when no longer needed. A bioreactor provides an appropriate environment and physiological signals during the development of tissues.

Rotating bioreactors were originally developed by NASA to culture cells on Earth in environments that simulate some aspects of microgravity. In one bioreactor configuration, cells are cultured in an annular space between two cylinders that are rotated as a solid body. In the present program, bioreactors of this configuration were adapted for tissue engineering by adjusting the speed of rotation to maintain large tissues (disks 5 to 10 mm in diameter and 1 to 5 mm thick) freely suspended during culturing. Engineered cartilage capable of withstanding mechanical loading and engineered cardiac tissue that contracted in response to electrical stimulation were grown in these reactors.

The cartilage-tissue-engineering model system developed in this program was selected for the first long-term cell-culture study in outer space, using bioreactors developed by NASA that were both rotated and perfused aboard U.S. space shuttles (STS-79 and STS-81) and the *Mir* space station (September 1996 to January 1997). Tissue mass increased on *Mir* as well as in control specimens cultured on Earth, and the component cells remained alive and metabolically active. Specimens grown on Earth retained their initial discoid shape, contained high fractions of glycosaminoglycan [GAG (a key cartilage component)] and had high compressive stiffnesses. In contrast, constructs grown on *Mir* tended to be smaller, to be more nearly spherical, and to have lower GAG fractions and compressive stiffnesses. This study proved the feasibility of long-term cell culture in outer space, and provided a basis for further studies aimed at developing countermeasures for prolonged human spaceflight.

Rotating bioreactors also provide favorable environments for engineering tissues on Earth. Engineered cartilage cultured 6 weeks in rotating bioreactors has slightly higher cellularity, 68 percent as much GAG, 33 percent as much collagen type II, and 19 percent of the compressive stiffness of native cartilage. Composites based on engineered cartilage were recently used to resurface knee joints in adult rabbits. After 6 months, engineered cartilage was preserved at the joint surfaces, where it remodeled to the dimensions of the surrounding host cartilage. The subchondral tissue remodeled into mineralized trabecular bone.

Engineered cardiac tissue cultured for 1 week in rotating bioreactors was found to exhibit 26 percent of the cellularity, 90 percent of the conduction velocity, and 65 percent of the maximum capture rate of native neonatal heart tissue. Electrical impulses were found to propagate between extracellular electrodes spaced up to 5 mm apart in tissue up to 0.1 mm thick, and the engineered cardiac tissue could be stimulated to contract at desired frequencies ranging from 60 to 270 beats per minute. However, the dimensions and mechanical properties of engineered cardiac muscle do not yet favor the use of this tissue to repair damaged cardiac tissue in experimental animals.

This work was done by Robert Langer, Lisa E. Freed, and Gordana Vunjak-Novakovic of Massachusetts Institute of Technology for **Johnson Space Center**.

In accordance with Public Law 96-517, the contractor has elected to retain title to this invention. Inquiries concerning rights for its commercial use should be addressed to

Lisa E. Freed, M.D., Ph.D.
Harvard-MIT Division of Health Sciences and Technology
MIT
Building E25-342
77 Massachusetts Avenue
Cambridge, MA 02139
Tel: (617) 253-3858
Fax: (617) 258-8827
E-mail: lfreed@mit.edu

Refer to MSC-22715, volume and number of this NASA Tech Briefs *issue, and the page number.*

END

04-30-02